Instrumentation of ATEK Flight Experiment

F. Klingenberg[1], F. Siebe[2], A. Gülhan[3], N. Wendel[4], R. Kronen[5],

1. Introduktion

The ATEK flight was successfully launched in the early morning of 13th July 2019 from Esrange Space Center near Kiruna (Sweden). ATEK used a two stage VSB-30 launcher with separation between μg-payload and 2nd Stage at 60 seconds. Both structures reached an apogee of approx. 240km. The 2nd stage had a flight time of approx. 500 seconds and landed without parachute at a speed of approx. 120 m/s. The μg-payload used a parachute system and reached the ground 800 seconds after launch.

To monitor structural health condition the hybrid structure and many parts of the 2nd stage was instrumented with pressure transducer, thermocouples, strain gauges, radiation sensors and special miniaturized infrared cameras. Here a special attention was paid to the motor adapter, tailcan and fin instrumentation. Fiber optic bragg gitters (FBG) were used to measure wall temperature at different location. The hybrid structure was part of the μg-payload.

The main achievement of the ATEK flight experiment was collecting valuable flight data from hybrid module and 2nd stage of the flight configuration. During ATEK flight Health Monitoring System allowed the measurement of aerothermal and mechanical loads on the hybrid payload structure, motor adapter, motor case, tailcan and fins along the complete trajectory. The DLR's Institute of Structures and Design in Stuttgart has developed a new payload structure using 'Automated Fiber Placement' (AFP) technique to manufacture a sounding rocket primary structure comprised of carbon fiber-reinforced thermoplastic (CF-PEEK) as interface an aluminum flange was used. In addition, a new nozzle consisting of CMC ad CFRP materials was developed for the 2nd stage motor, Although this nozzle passed the ground qualification tests, it wasn't used for the flight for safety reasons. To monitor these structures also a new distributed data acquisition system was developed [2].

[1] *Supersonic and Hypersonic Technologies Departments, DLR, Cologne, Germany, florian.klingenbger@dlr.de)*
[2] *Supersonic and Hypersonic Technologies Departments, DLR, Cologne, Germany*
[3] *Supersonic and Hypersonic Technologies Departments, DLR, Cologne, Germany*
[4] *Supersonic and Hypersonic Technologies Departments, DLR, Cologne, Germany*
[5] *Supersonic and Hypersonic Technologies Departments, DLR, Cologne, Germany*

Fig 1. ATEK team after the flight preparation of the second stage S30 motor

2. Instrumentation

2.1. Instrumentation Overview

The ATEK Health Monitoring System consists of main systems. The first system is part of the hybrid module. Here the monitoring system has to acquire structure strain and temperature. For this goal strain gauges, thermocouples and fiber optic sensors (FOS) are used. The second part is the instrumented 2nd stage reentry configuration. Here different critical parts are monitored by pressure transducers, strain gages, thermocouples, heat flux sensors, miniaturized infrared cameras, fiber optic sensors and radiometers.

2.2. Hybrid Structure Module

The DLR Institute of Structures and Design developed the hybrid structure module. This structure has a diameter of 435mm with a wall thickness of 4,5mm and is made of PEEK/CFK. As interface to the adjacent modules an alumina RADAX flange is used [3].
To monitor the structure conditions strain gauges, thermocouples and fiber optic sensors are implemented (Fig 5 andTable 1). For strain measurement strain gauges with three measuring grids arranged in 0°/45°/90° are placed each 90° in the middle of the PEEK/CFK segment. The electrical configuration of each strain gauge is a wheatstone quarter bridge. To compensate the temperature shift, each measuring point has one additional thermocouple. The structure temperature is measured by Ø 0.5mm thermocouple mounted approx. 2mm deep to the structure (Fig 4). These thermocouples are arranged five times in axial direction and four times in radial direction. In addition temperature measurements were also carried out using fiber optic sensors. Here the fiber-bragg-gratings (FBG) are orientated similar to the thermocouple, one line in axial direction and two lines in radial direction at 33% and 66% of the segment length. To acquire all this sensor information two different data acquisition systems are implemented in this structure. The first one acquires all electrical signals, converts them and stores them on an onboard data storage unit with up to 1 kSamples/second. Part of the data with a lower bandwidth is transmitted during complete flight via telemetry directly to ground. The second system is the FOS interrogator. Here the three FBG fiber lines convert structure temperatures to wavelength information at the sampling rate is up to 2 kSamples/second. The interrogator also stores the full data rate on onboard and transmits it with a lower bandwidth via telemetry to ground. Both systems are powered during the whole flight by the rocket service system.

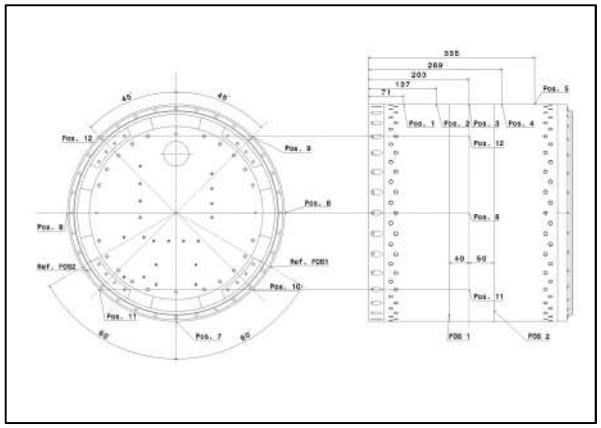

Fig 2. Sensor Position Hybrid Container Module

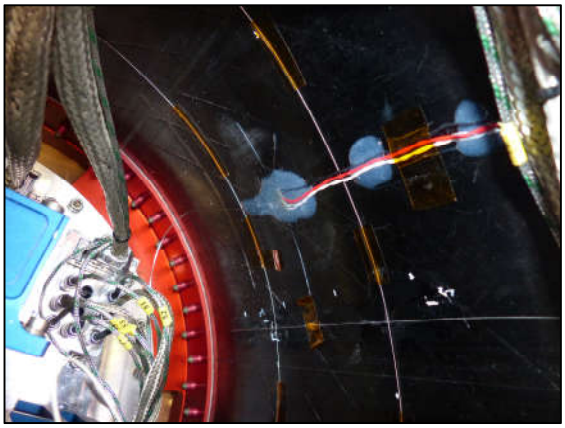

Fig 3. Instrumented Hybrid Structure

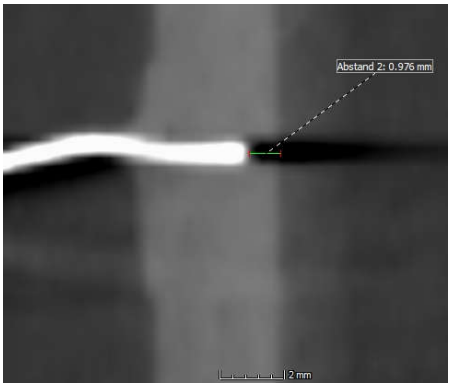

Fig 4. CT of mounted Thermocouple

Fig 5. Sensor Position Hybrid Container Module

Table 1. Sensor declaration

Position (Fig 5)	Sensor Group	Sensor Type
1-12	Thermocouple	Sheath thermocouple Ø0,5mm Type K
9-12	Strain Gauge	0°/45°/90° DMS Grid
FOS 1-4	FOS Line	6x Fiber Bragg Gratings

2.3. Second Stage Instrumentation

The 2nd stage instrumentation includes motor adapter, motor case, tailcan, fins and nozzle. Here temperature, structure strain, pressure, heat flux and plum radiation are measured. The corresponding data acquisition system to acquire the sensor data is divided in two main parts. One part is placed in the motor adapter and the second part is integrated into the tailcan. A connection to the rocket service module was only during the first flight phase until the separation of µg-payload and 2nd stage possible. For this reason, the data acquisition system needs its own power supply in motor adaptor and tailcan. An additional feature is its data storage capability. To reduce the impact acceleration, for case without parachute assisted landing, all storage units have an impact resistance design and are placed in the taican. This design is for electrical data acquisition, FOS interrogator and infrared cameras.

Motor Adapter and Motor Case

The motor adapter instrumentation includes pressure ports for a flush air data system, two in-house developed heat flux sensors based on Typ E coaxial thermocouples and Typ K structure thermocouples. The thermocouples measured the efficiency of the cork thermal protection system. Therefore, two stripes with different width of 25mm and 50mm are non-protected with cork. To measure the motor case temperature two FOS fiber lines are implemented between 505mm and 575mm downstream of the interface to motor adapter. A video camera is mounted on the front bulkhead, which monitor the separation process end reentry phase.

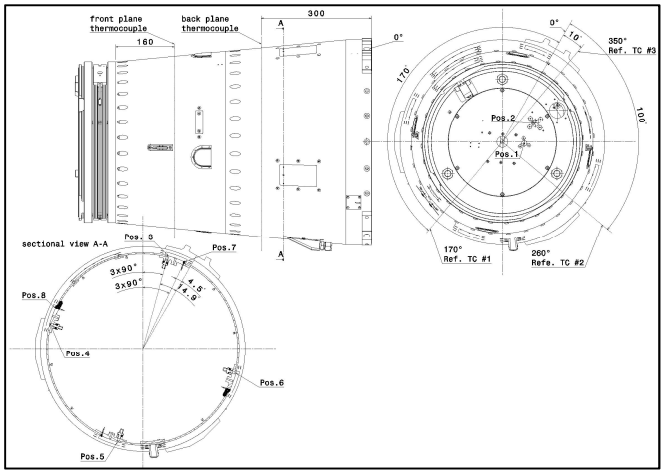

Fig 6. Sensor Position Motor Adapter (MA)

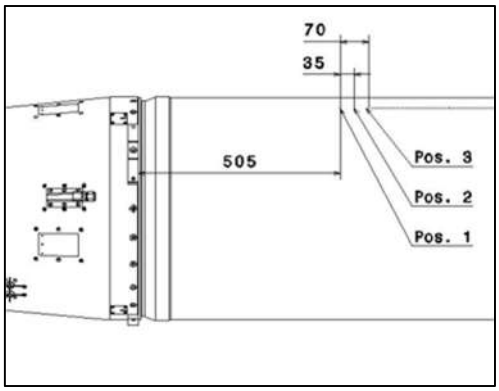

Fig 7. Sensor Position Motor Case (MC)

Table 2. Sensor Declaration Motor Adapter

Position (Fig 6+Fig 7)	Sensor Group	Sensor Type
1,3,5 (MA)	Pressure Sensor (Absolut)	Kulite XTEL-190L-25A
2(MA)	Video Camera	Split 2
3+4,5+6 (MA)	Pressure Sensor (Differential)	Kulite XTE-190LM-+/-5D
Ref TC #1-3 front+back (MA)	Thermocouple	Type K
1,2,3 (MC)	Temperature	Fiber Bragg Gitter

Tailcan

The tailcan instrumentation includes pressure sensor, thermocouples and strain gauges. Furthermore two infrared cameras are embedded. The first one measure the fin surface temperature and the second one measures the outer nozzle wall temperature. Type K thermocouple are mounted with cable lugs on the inner tailcan surface. The orientation is in axial direction over the complete length and at the tailcan aft exit plane. One pressure sensor measures the internal tailcan pressure. Next to the fin shoes strain gauges are implemented to measure the interaction between tailcan and fin during deflection. Near to the three guiding pins from the interstage adapter (S31-S30), also strain gauges are implemented; these measure the thrust of first stage and monitor the symmetry of separation process.

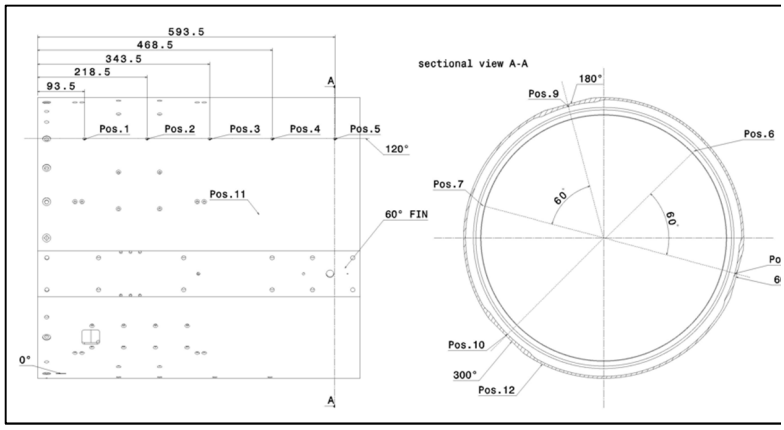

Fig 8. Sensor Position Tailcan

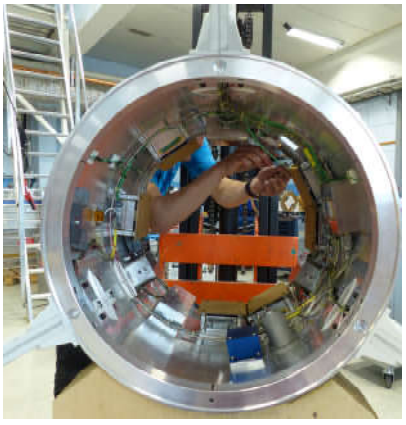

Fig 9. Instrumented Tailcan

Table 3. Sensor Declaration Motor Adapter

Position (Fig 8)	Sensor Group	Sensor Type
01…10	Thermocouple	Type K
8,9,10	Strain Gauges	HBM

11	Pressure Sensor (Absolut)	Kulite XTEL-190L-25A
12	Strain Gauge	HBM DY43-6/350

Fin

One fins of the S30 motor is instrumented with thermocouples, strain gauges and pressor sensors (Fig 10 ??). Thermocouples are implemented in the stainless-steel leading edge and in the fin tip. Here they are fixed on the inner surface. Strain gauges are implemented on the fin structure near to the fin root. The electrical configuration is Wheatstone full bridge. To monitor the thermal condition here also type K thermocouples are implemented. To measure the fin surface pressure, two pressor transducers (absolute and differential) are integrated into the fin structure. The other two fins are equipped with multiband radiometers in the aft to measure radiation of plume.

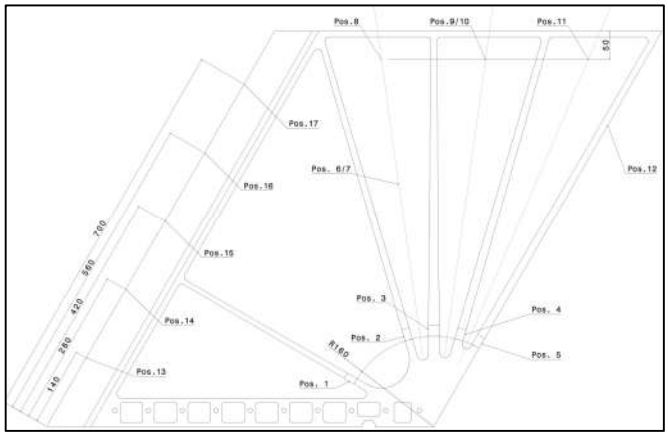

Fig 10. Sensor Position Fin

Fig 11. Instrumented Fin

Table 4. Sensor Declaration Fin

Position (Fig 8)	Sensor Group	Sensor Type
01…5 (FBS1…FBS5)	Thermocouple	Type K
11	Pressure Sensor (Absolut)	Kulite XTEL-190L-25A
12	Strain Gauge	HBM DY43-6/350

Nozzle

In the ATEK project a new nozzle consisting of CMC and CFRP structures was developed to replace the original S30 nozzle and to reduce the structural mass. During the qualification process of the nozzle some cracks occur. For safety reason the original nozzle was used for the ATEK flight. To qualify and monitor the new nozzle several thermocouples and strain gauges were foreseen. Also, an IR camera should monitor the outer nozzle wall temperature. To have comparative wall temperature measurements the thermocouples were used on the original S30 nozzle. The IR camera, which was calibrated for measurement of the wall temperature distribution of the new nozzle, was kept in the tailcan for the flight with the original nozzle. But, because of its titanium flange (instead of the CFRP material of the new nozzle) the data was strongly manipulated by reflections. But this flight opportunity is used to qualify the IR camera design.

3. Flight Experiment Description

The ATEK flight experiment was launched on 13th of June 2019 from Skylark Tower of launch side Esrange (Sweden) and reached an apogee of approx. 240km. The first stage S-31 booster burned for 13 sec. At a flight time of 15 sec second stage ignition took place and burned until 45 sec. After 57sec the Yo-Yo system reduced the roll-rate nearly to zero and at 60 sec the µg-payload was separated from the S-30 motor

Fig 12. ATEK flight configuration launching from the Skylark tower of Esrange

Table 5. ATEK Flight Events

Time	Event
T0s	Liftoff/Ignition 1st stage
T+11,5s	Tailoff 1st stage
T+12,0s	Acceleration = 0m/s² (Altitude 3,7km)
T+15s	ignition 2nd stage
T+35s	Tailoff 2nd stage
T+43,5s	Acceleration = 0m/s² (Altitude 41km)
T+57s	Yo-Yo De-spin
T+60s	Motor separation
T+250,8s	Apogee 238,8KM
T+619,5s	Impact 2nd stage (@67km downrange)
T+795,3s	Landing µg-Payload (@68km downrange)

4. Results

4.1. Hybrid structure

After flight all measurement systems and the structure itself are in very good conditions (Fig 13). The surface color of cork thermal protection system after flight indicated high environmental temperatures during flight (Fig 14). The data acquisition system for sensor signals run along the complete flight and show good results. Only the FOS system stops data recording 85 seconds after lift-off because of an internal failure. The temperature profile of sensors HY2_TC01 and HY2_TC04 mounted inside CFRP structure under the cork layer show the main heating process during the atmospheric ascent and descent phase (Fig 15). The difference between two signals is caused by the sensor depth inside the material. Also, the comparison to the FOS system gives good results. The difference during the first 45 sec. is caused by the high motor induced vibrations. After this phase the temperature is lower because the mounting position is on the inner wall.

Fig 13. Microgravity experiment section MAPHEUS 8 with integrated hybrid module after ground impact

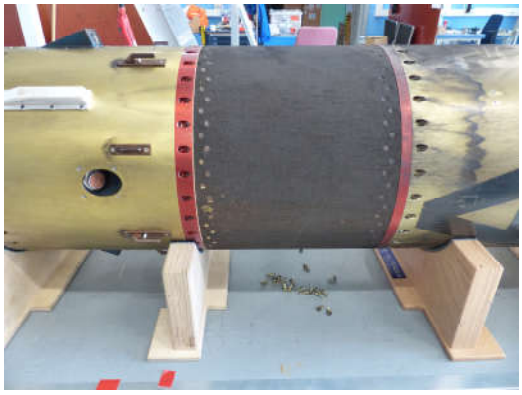

Fig 14. Hybrid Structure after Flight

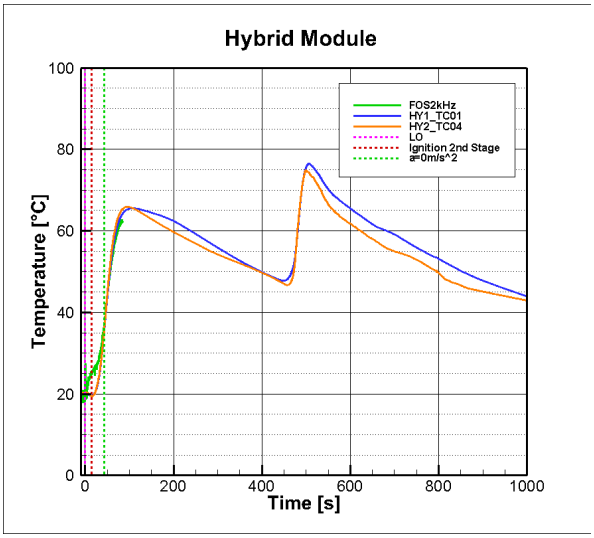

Fig 15. Hybrid Structure Wall Temperature

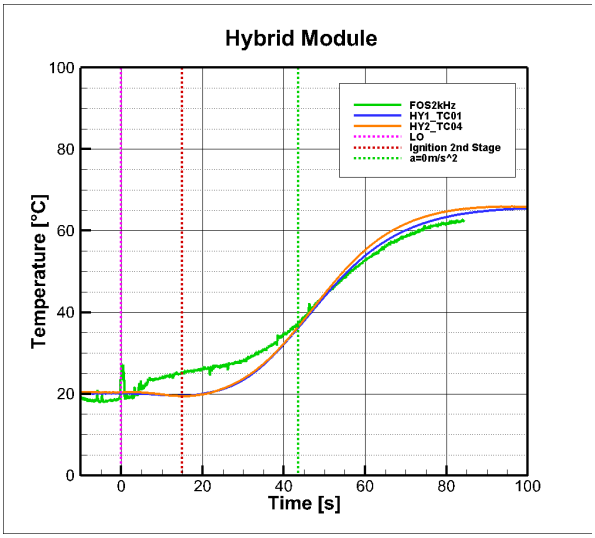

Fig 16. Ascent Phase

4.2. Second stage Instrumentation

As planed the S-30 configuration separate 60 seconds after lift-off from µg-payload and acquire suitable date during the whole flight. During decent, after approx. 470 sec, the fins didn't survive the high aerothermal loads and were fully destroyed (Fig 17 left). The S-30 stage had a hard impact with approx. 120 m/s after 619,5 s flight time. Fig 17 shows the main structure parts after impact. The crash resistant data storage units were still in very good condition. Only a few pins of the D-Sub connector were bended. All data could be read without any problem.

Fig 17. Loss of Fins, view from µg-Payload (left), Motor Adapter after impact(middle-left), S-30 Motor after Impact (middle-right), Tailcan after Impact (right)

Motor and Motor Adapter

Fig 18 shows the absolute pressure history along the flight. One of the tubes to the differential pressure transducers failed. The figure shows also the high dynamic loads during reentry. After loss of fins the motor goes into a flat spin. This process is also visible in the motor adapter wall temperatures (Fig 19). It seems that thermocouple MA_TC01 was during the descent phase on the wind side. Loss of TC2_TC2 is given by the loss of fins, this sensor was rooted to the data acquisition system implemented in the tailcan. The different temperatures during ascent phase between MA_TC01 MA_TC02 und TC2_TC11 are linked to the different width of cork free stripes.

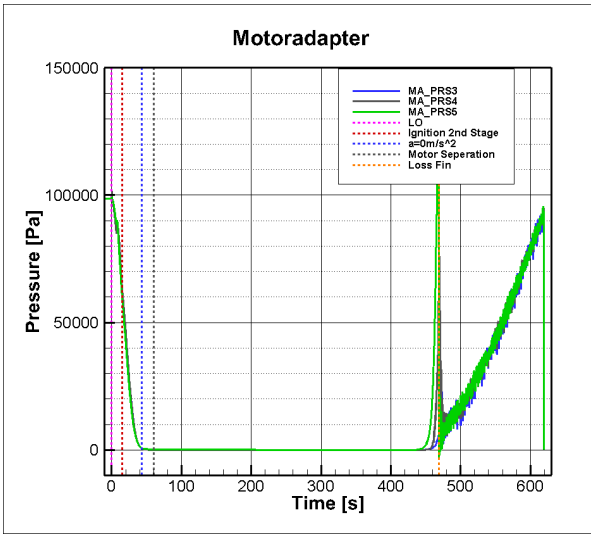

Fig 18. Measured pressure history on motor adapter wall

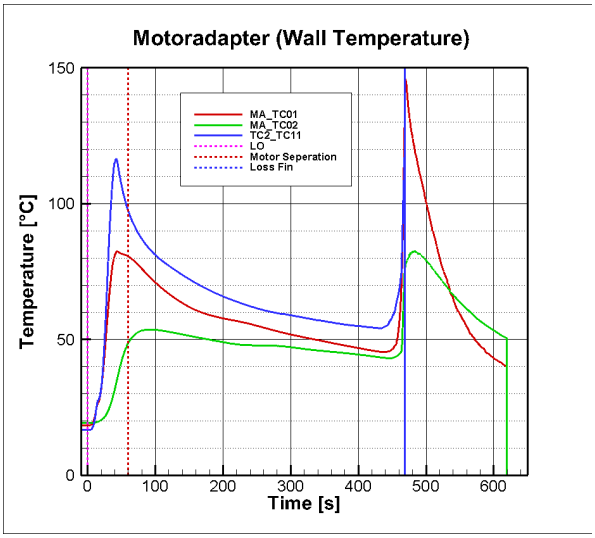

Fig 19. Measured temperature history in motor adapter wall

Tailcan

The tailcan data acquisition system provide data until impact. In case of the loss of fins some sensors which are rooted to the same data acquisition board are lost with the fins. This depends on shorten circuit. The inner tailcan pressure show all flight events (Fig 20). At 12 sec the passive separation is visible with ignition of 2nd stage at 15 sec and pressure fluctuation during burn phase. Short pressure peeks at the beginning of descent phase could be given by roll overs of 2nd stage. Tailcan thermocouples show during most of the time of burning phase nearly the same temperature (Fig 21). Thermocouple TC1_TC5 is very close to the nozzle exit and didn't survive. The gradient in temperature could be caused by radiation and the distance to the hot nozzle. The strain profile (Fig 22) in the tailcan aft has good correlation to the thrust profile of S-31 booster. Fig 23 top show am infrared image of the metallic cover of the original S30 nozzle.

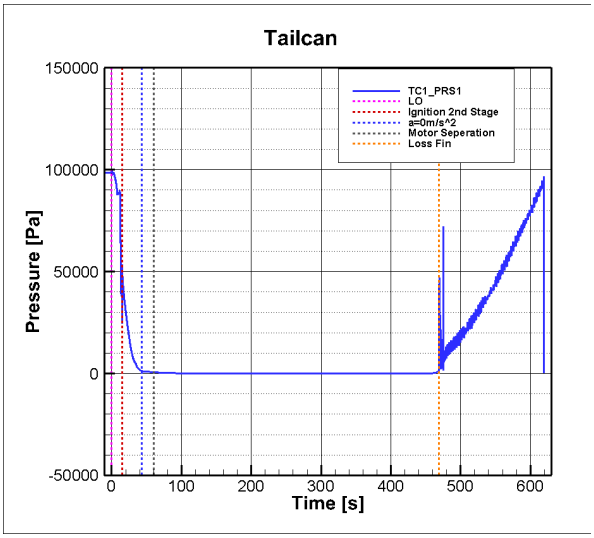

Fig 20. Measured pressure history inside tailcan

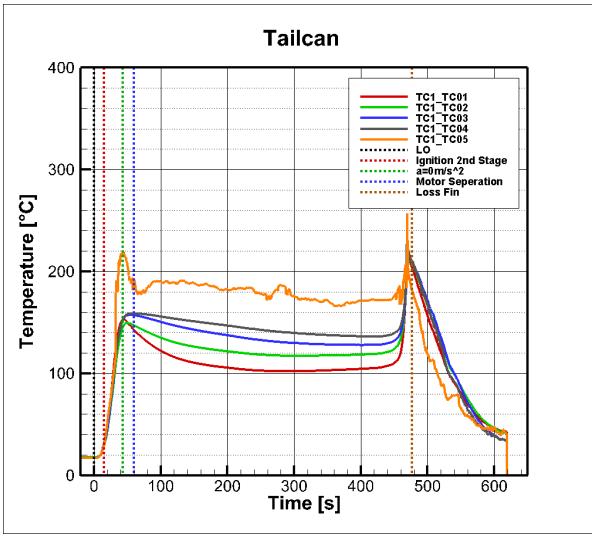

Fig 21. Measured inner tailcan surface temperature history

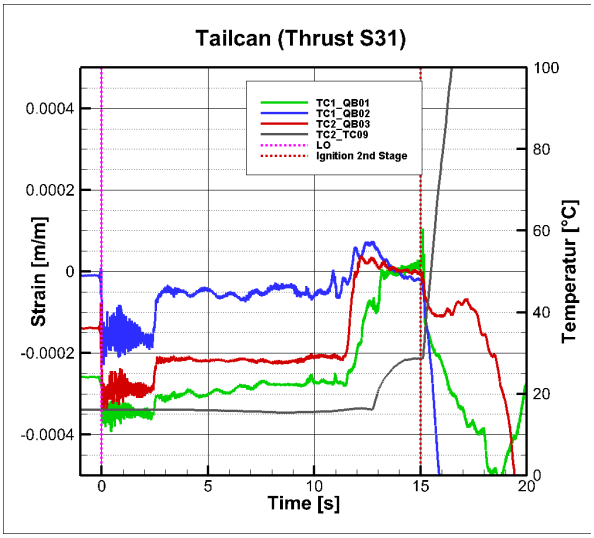

Fig 22. Thrust induced strain in S-30 tailcan

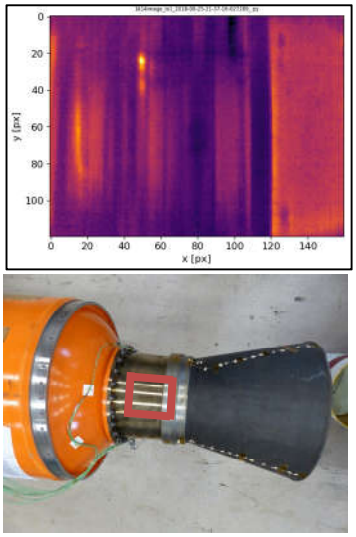

Fig 23. Nozzle Flange IR Image(top) ROI IR Camera (bottom)

Fin

The fin measurement shows very good data until they were destroyed. During ascent phase a lot of dynamics are visible. Fig 25 shows the measured pressure profile during ascent. The fluctuations in the pressure signal of the differential sensor FN2_PRS2 could be the result of the combination of spinning motion and angle of attack of the vehicle. The signal drift during ascent and descent is caused by thermal effects in the sensor. Strain measurements shown in Fig 26 and Fig 27 indicate a mechanical deformation resulting in the offset after thrust phase. The drift apart between ascent and descent could occur by thermal stress reaction after deformation. An interesting point is at T+20s here the high strain loads are not linked to the pressure measurement. The temperatures measured with thermocouples TC02, TC03 and TC04, which are positioned in the middle section of the fin leading edge, follow similar evolution over the complete ascent and flight time (Fig 28). The maximum fin leading edge temperature is achieved at the flight time point of 44 seconds and is near to the material operating temperature. The further decrease of the temperature is caused by radiative cooling of the fin structure. The temperature of the thermocouple TC05 has a lower peak value during ascent and remains below temperatures of other thermocouples along the complete flight phases. An imperfect contact of the thermocouple TC05 to the structure may be responsible for this behavior. A closer look to the ascent phase confirms this hypothesis (Fig 29). TC05 data shows a delayed response to aerothermal heating. A similar tendency is observed in the response of TC01, which is mounted to the interface between the fin and tailcan. The radial distance from the interface line is 120 mm. It has to be checked whether this sensor was exposed to the boundary layer flow or separated flow. The change in temperature increase beginning from 28 sec is caused by erosion of the thermal protection layer at the leading edge. Fig 30Fig 30 shows measured moderate temperatures on the fin sidewall during the complete flight.

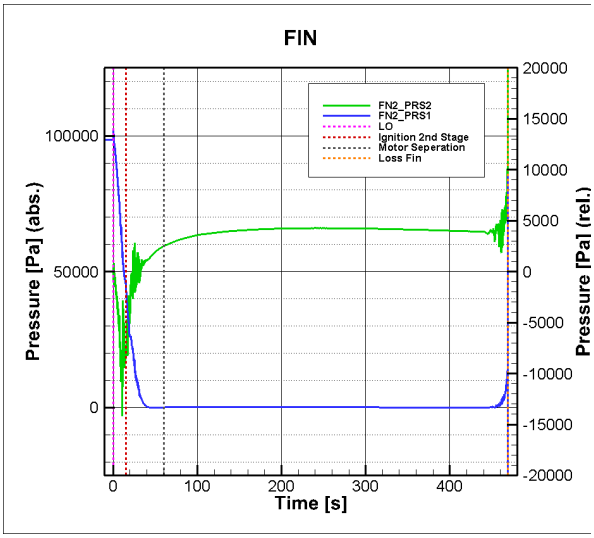

Fig 24. Measured fin surface pressure history

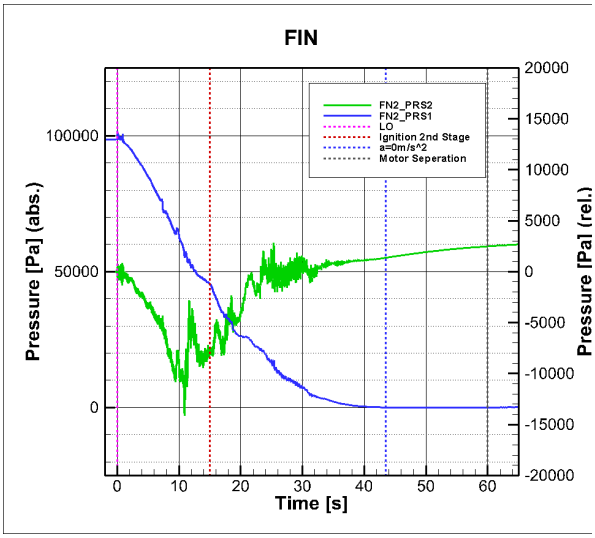

Fig 25. Measured fin surface pressure history during ascent

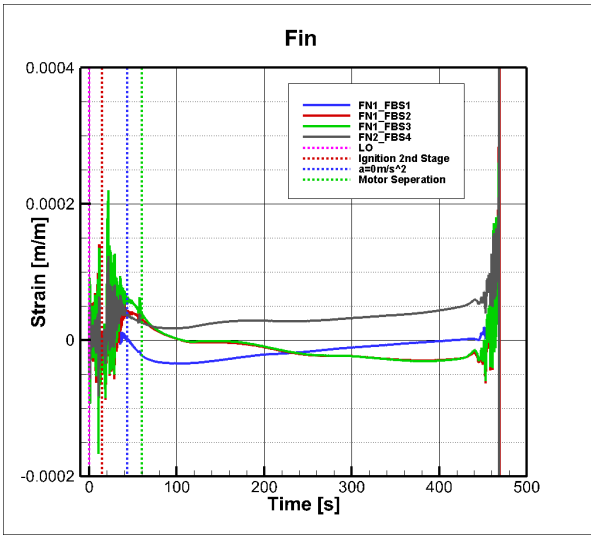

Fig 26. Measured internal fin strain history

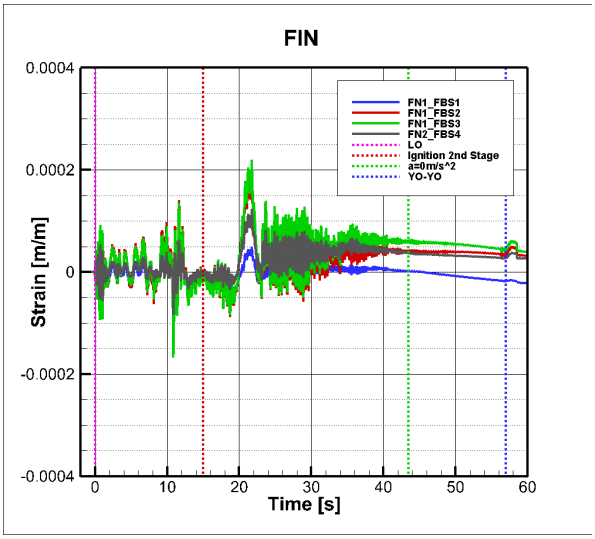

Fig 27. Measured internal fin strain history during ascent

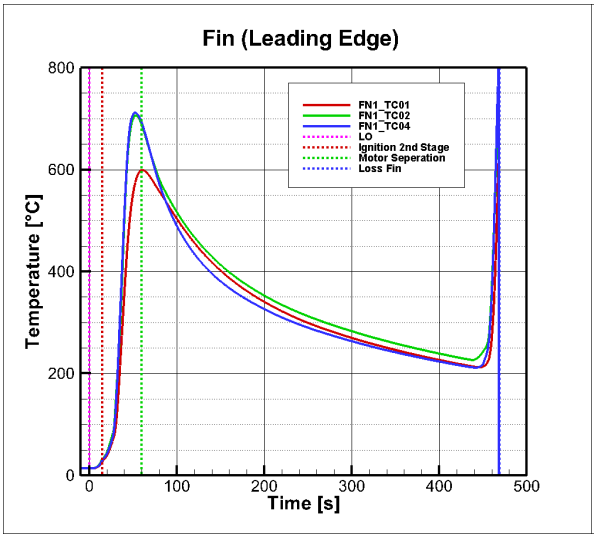

Fig 28. Measured fin leading edge temperature history

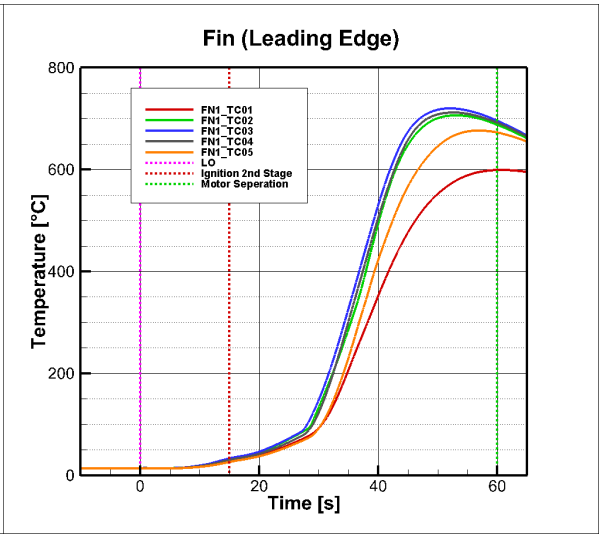

Fig 29. Measured fin leading edge temperature history during ascent

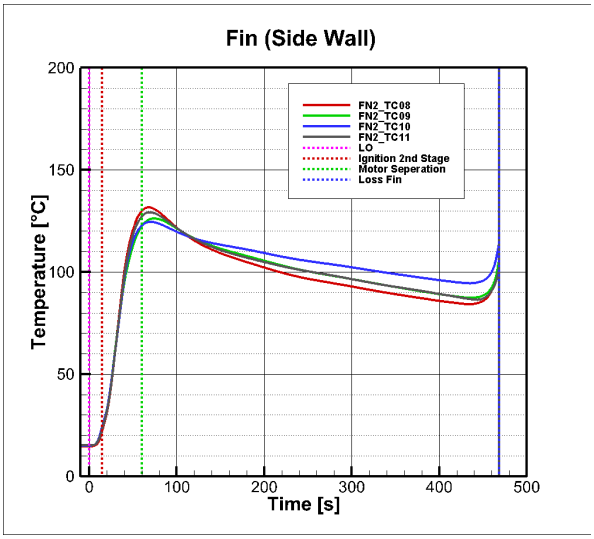

Fig 30. Measured fin side wall temperature history

5. Conclusion

The different components of ATEK health monitoring system collected very good flight data during complete flight. All data fits very well to the flight events and shows theirs dynamic. The measured loads during ascent are in an expected range. Only the thermocouples of the fins leading edge shows high values with are near to the material operating limit. During uncontrolled descent flight the loads on the fins are to high and they are destroyed. Here the data sampling rate is to low to understand the mechanism exactly. The valuable expertise gained during ATEK project was used to design the STORT experiment [4]

References

1. A. Gülhan, F. Klingenberg, F. Siebe, A. Kallenbach and I. Petkov; Main Achievements of the Sounding Rocket Flight Experiment ATEK, IAC, Dubai, October 25-29, 2021, IAC-21,D2,6,4,x62713
2. F. Siebe, F. Klingenberg, R. Kronen, A. Gülhan; Autonomous Data Acquisition System for the Hybrid-Structure and the 2nd Stage of the Sounding Rocket flight Experiment ATEK, HiSST:

2nd International Conference on High-Speed Vehicle Science Technology, 12-15 September 2022, Bruges, Belgium.

3. Chadwick, P. Dreher, I. Petkov, S. Nowotny: A. Fibre-reinforced Thermoplastic Primary Structure for Sounding Rocket Applications, SAMPE Europe, Nantes, France, 2019.
4. A. Gülhan, D. Hargarten , F. Klingenberg , F. Siebe , G. di Martino , T. Reimer; Main Results of the Hypersonic Flight Experiment STORT, HiSST: 2nd International Conference on High-Speed Vehicle Science Technology, 12-15 September 2022, Bruges, Belgium.